3D seismic waveform of channels extraction by artificial intelligence

Dawei Liu[1], Xiaokai Wang[1], Wenchao Chen[1], Yanhui Zhou[1],Wei Wang[2],Zhensheng Shi[1],Cheng Wang[3],Chunlin Xie[3]*
[1]Xi'an Jiaotong University, National Engineering Laboratory for Offshore Oil Exploration, Xi'an, China
[2]DataYes, Shanghai, China [3]Daqing Oilfield Company Ltd., Daqing, China

Summary

Channels are important exploratory objectives in reflection seismology. Geologic bodies such as channels and point bar produce the laterally-inhomogeneous geological body (LGB) waveform response in seismic sections. Due to the limitation of the seismic signal's resolution, it always makes detailed interpretation challenging when channels are seriously affected by the signals of overlying strata or the underlying strata. We propose a method based on convolutional neural networks (CNN) to extract LGB waveform response from the raw seismic dataset. We divide raw seismic data volume into training data volume and testing data volume. Our CNN is trained with selected training data volume in which the LGB waveform response is clear. Then, we test the model by using the testing data volume in which the LGB waveform response is seriously covered. In order to utilize more information from different directions, we feed a three-dimensional (3D) training dataset to the network. Two 3D field seismic data examples verify the validity of our proposed method. After extracting LGB waveform response by using our method, the channel structure becomes clearer, which is very helpful to reduce the texture interpretation's uncertainty.

Introduction

The sandstone within channel facies is one favorable reservoir. The identification of channel sand bodies is very difficult due to the low seismic resolution. Quickly and accurately identifying channel sand body is essential in petroleum exploration, which will increase the drilling success rate and reduce the investment risk.

In order to accurately identify channel sand body, many methods for imaging small-scale structures, such as edges and internal architecture of the stratigraphic targets, have been proposed. Seismic attributes and spectral decomposition are mostly used methods. Gray level co-occurrence matrix (GLCM) was first proposed by Haralick and Shanmugam (1973). It transforms the gray value of a two-dimensional image into texture information. Using the seismic texture analyzing method based on GLCM to analyze the time and space waveform characteristics of seismic reservoirs is an effective way to identify sedimentary characteristics of sand bodies (Gao, 2003, Chi et al., 2018). Other seismic attributes, such as sweetness attributes based on instantaneous frequency (Hart, 2008) and similarity attribute based on gradient structure tensor (Wu, 2017), have been proposed for helping channel identification. Coherence measure, which measured changes in waveform quantitatively, was used to characterize the edges of stratigraphic units (Marfurt and Kirlin, 2000). Besides, spectral decomposition with transforms that decompose seismic data in scale and orientation have also been used to highlight channels and allow better imaging channel details such as steerable pyramid (Mathewson and Hale, 2008) and shearlet transform (Karbalaali et al., 2017).

Manual interpretation of the channels is one time-consuming job which requires a skillful expert with special training. Schwab et al. (2007) studied the channel stacking architecture of low-accommodation space and high-accommodation space. Suarez et al. (2008) calibrated the response of different attributes based on a well-understood reservoir. In recent years, machine learning has made a big development in the field of image recognition due to its powerful ability of feature extraction. Many researchers introduce deep learning into seismic signal interpretation. Araya-Polo et al. (2017) proposed a deep learning method by integrating Wasserstein loss function to identify fault automatically. Zhao (2018) successfully applied encoder-decode CNNs to classify seismic facies and compared the results of the patch-based model and the encoder-decoder model. Pham et al. (2018) applied an encoder-decoder network for channel detection and found the network can be transferred to identify the channel bodies in the field dataset with training on the synthetic dataset.

Although so many sophisticated analyzing methods for channel identification have been proposed, it is important to mention that the raw seismic data waveform response itself is a key factor that will determine the resolution and quality of the seismic attribute response. Wang et al. (2011) proposed a method to separate the waveforms response of channel architecture from 3D seismic data with the help of morphological component analysis (MCA). Proper choice of prototype waveform dictionaries that can provide sparse representation to target signal's morphology is crucial to the success of the above method. Inspired by Wang et al. (2011) and the fact that neural networks have strong feature learning ability, we try to propose an approach using the deep neural network to learn the features of channel's seismic waveform response and separate the meaningful geological targets from 3D seismic data.

Method

Training data

10.1190/segam2019-3216216.1

Our training dataset consists of the raw seismic dataset and corresponding label dataset. Geologic bodies such as channels and point bar produce LGB waveform response in seismic sections. We regard LGB waveform response which is extracted by using the MCA-based feature extraction algorithm (Wang et al., 2011) from raw seismic data as the ground-truth labels. The MCA based on sparse representation was first proposed for separating texture in natural images and gradually extended to separate several signal components which have morphology differences.

MCA theory requires that the initial signal must consist of different morphological components. Therefore, we simply suppose the raw seismic data comprises the LGB waveform response and stable sediments (SS) waveform response. The LGB waveform response has a small spatial distribution range, while the corresponding waveform response of SS has a wide-spread spatial distribution range and stable waveform. The difference in the spatial characteristics of these two components is distinguished apparently. Based on the above-mentioned hypotheses, a vertical section s of 3D raw seismic data along the inline or crossline direction is modeled as follows:

$$s = s_p + s_c + n, \tag{1}$$

where s_p and s_c respectively indicates LGB response and SS response, and n indicates a Gaussian noise with zero mean and a standard deviation σ. Therefore, the above feature extraction problem based on MCA can be formulated as the following optimization problem form:

$$\underset{\{\mathbf{x}_p, \mathbf{x}_c\}}{\arg\min} \|\mathbf{x}_p\|_1 + \|\mathbf{x}_c\|_1, \quad \text{s.t.} \quad \|\mathbf{s} - \mathbf{\Phi}_p \mathbf{x}_p - \mathbf{\Phi}_c \mathbf{x}_c\|_2^2 \le \varepsilon, \tag{2}$$

where $\mathbf{\Phi}_p$ and $\mathbf{\Phi}_c$ are sparse representing dictionaries for s_p and s_c respectively, $\mathbf{x}_p$ and $\mathbf{x}_c$ are sparse representation coefficient of corresponding dictionary $\mathbf{\Phi}_p$ and $\mathbf{\Phi}_c$. Two-dimensional undecimated wavelet has the strong ability to describe complex point structure and is chosen as $\mathbf{\Phi}_p$ for representing LGB waveform response. The curvelet transform has an excellent multi-scale and multi-directional resolution. Thus, the curvelet transform is chosen as $\mathbf{\Phi}_c$ for representing SS waveform response. Finally, the block coordinate relaxation algorithm is applied to solve the optimization problem in Equation (2) and extract LGB seismic waveform response from raw seismic data.

The above separation model is built up on the basis of 2D vertical sections. Channel sand body in a seismic section is considered as an interruption of reflection continuity while their detection is easier in time or horizon slices of the 3D seismic dataset. In order to introduce more information and improve extraction accuracy, we build training dataset in three dimensions by cutting raw 3D seismic data and corresponding LGB waveform response into small cubes.

In addition, as shown by yellow ellipses in the seismic section (Figure 1a), LGB waveform response can be clearly observed in shallow layers. As shown in Figure 1b, the response of LGB waveforms is also clear in the time slice of 0.046s. As shown by the yellow boxes in Figure 1a, the sandstone underlying sand-shale is the reservoir in this data. However, due to the strong reflection interface of sand-shale, it is impossible to clearly depict the weak-energy LGB waveform response in the deep layer. In order to make the network accurately extract the features of LGB waveform response, we use shallow seismic data with distinct LGB waveform response for training and apply well-trained network for extracting LGB waveform response in deep layer where LGB waveform response is difficult to identify.

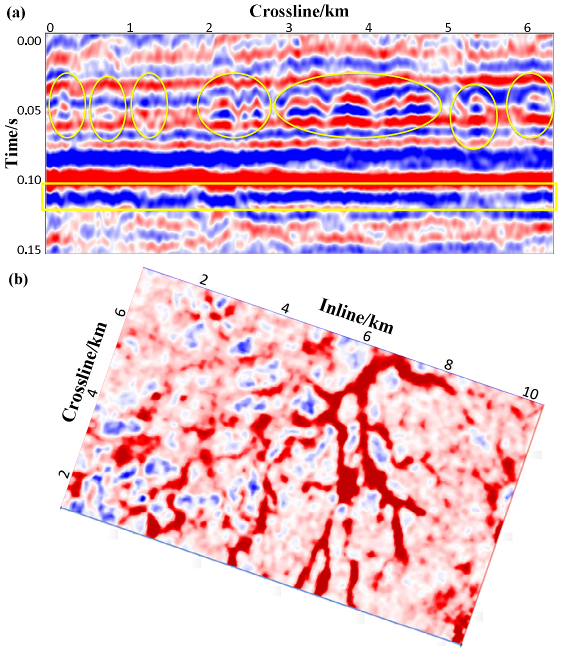

Figure 1: Raw seismic data. **(a)** Raw seismic section. The channel structures in shallow layer (indicated by yellow ellipses) are clear. However, the deep layer data are covered by the strong reflection layer, which makes it impossible to clearly depict the weak-energy LGB waveform response. **(b)** A time slice of 0.046s for training.

Network architecture and model training

The input of our proposed CNN is the raw 3D seismic data volume $\mathbf{s} = \mathbf{p} + \mathbf{c}$, where $\mathbf{p}$ is the LGB waveform response and $\mathbf{c}$ is SS waveform response. The training dataset contains a number of pairs of 3D seismic data cubes $\mathbf{s}$ and

10.1190/segam2019-3216216.1

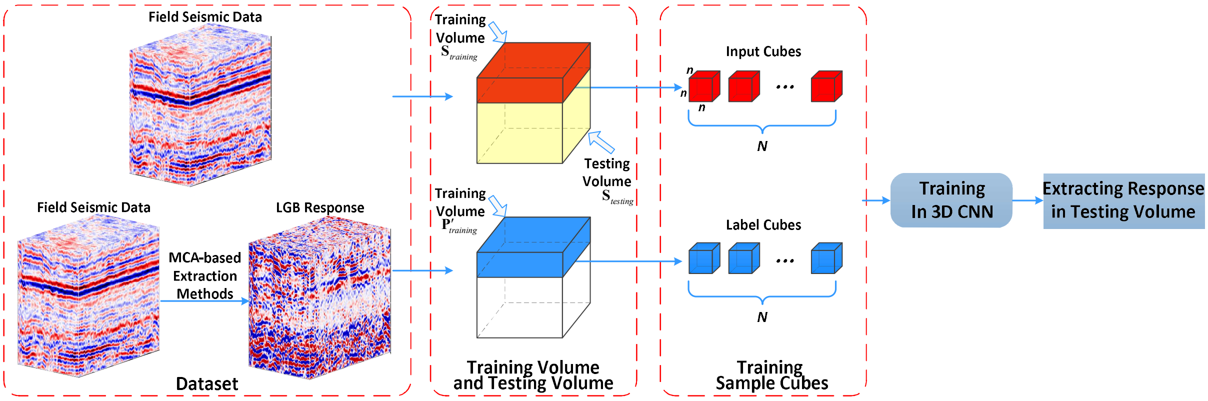

Figure 2: Proposed workflow based on 3D CNN for extracting LGB response. The training data are extracted as a subset from the field seismic data and the corresponding LGB response extracted by MCA-based method.

their corresponding ground-truth label $\mathbf{p}'$. We utilize CNN to learn a residual mapping $\Re(\mathbf{s}) \approx \mathbf{c}$ which transforms the input raw seismic data to SS waveform response. We can obtain the network output $\mathbf{p} = \mathbf{s} - \Re(\mathbf{s})$, which is regarded as the LGB waveform response. We utilize the averaged mean square to measure the error between raw seismic data and LGB waveform response. The corresponding formula can be written as:

$$l(\mathbf{\Theta})=\frac{1}{2N}\sum_{i=1}^{N}\left\|\Re(\mathbf{s}_i;\mathbf{\Theta})-(\mathbf{s}_i-\mathbf{p}'_i)\right\|_F^2 \tag{3}$$

We utilize the back-propagation method (Rumelhart et al., 1986) to get a locally-optimal of trainable parameters $\mathbf{\Theta}$ after iterative training.

Figure 3 shows the detailed architecture of the proposed 3D CNN for extracting LGB waveform response. Our proposed CNN regression model is structured into three stages. The first stage is one convolutional layer. Following the experimental parameter setting in VGG-net (Simonyan and Zisserman, 2014), we choose the size of convolutional kernel to be $3 \times 3 \times 3$ and delete all pooling layers to keep the network output same size as the input size. The second stage is composed of fifteen convolutional layers, each of which is followed by a batch normalization layer. Batch normalization is adopted for reducing covariance shift and accelerating training convergence, which will improve the extraction accuracy of our method. The third stage is composed of one convolutional layer.

In the process of convolution calculation, the data on the boundary should also be convoluted so that we need to choose a padding approach that can satisfy this problem from the existed padding strategies. In the end, we found that zero padding can meet our requirements and will not bring interference information.

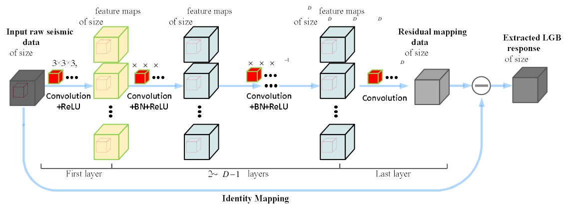

Figure 3: Architecture of the proposed 3D CNN for LGB features extraction.

Examples

Firstly, we apply our proposed method to a subvolume of a field dataset from an oil field in Eastern China with 514 inlines, 301 crosslines, and 401 time samples. The data volume has a time sampling interval of 1 ms, and inline and crossline spacing of 20.0 m. In deep layer time slice, as shown in Figure 4a, we can observe the complex reflection features which make it difficult to clearly characterize the channel characteristics of some weak energies. Figure 4b shows the LGB seismic waveform response extracted by the MCA method in 2D. It can be observed that the LGB seismic waveform response which could not be displayed in raw seismic data can now be observed in the time slice. Figure 4c shows our network output of same time slice after training in 3D. As illustrated in Figure 4, it can be seen that some of the partially observed channels in the raw data can be presented more clearly. Moreover, more LGB seismic waveform response is revealed compared to Figure 4b.

Then we apply our proposed method to another dataset of an oil field which is 100 kilometers away from the previous one with 681 inlines, 401 crosslines, and 256 time samples. As shown by the black circles in Figure 5, the LGB wave response based on our method has more prominent channel details compared with MCA-based method.

Conclusions

In this abstract, we propose one LGB waveform response extraction method based on deep learning. The convolutional regression model is trained in shallow layers of seismic data volume where LGB waveform response is clear and tested in deep layers of seismic data volume where LGB waveform response is seriously covered. Two examples of field seismic data show that our model successfully extracts LGB seismic waveform response. Compared with the traditional extraction method based on MCA, our method can reveal more LGB waveform response with training in 3D. We believe the proposed method has a high potential for subsequent quantitative analysis and reservoir modeling.

Acknowledgments

The research was funded by National Natural Science Foundation of China (41774135, 41504092, 41504093), China Postdoctoral Science Foundation (2016T90925, 2015M572567), National Key Research and Development Program of China (2017YFB0202902), and the Fundamental Research Funds for the Central Universities. We would like to thank Daqing oilfield for providing the dataset.

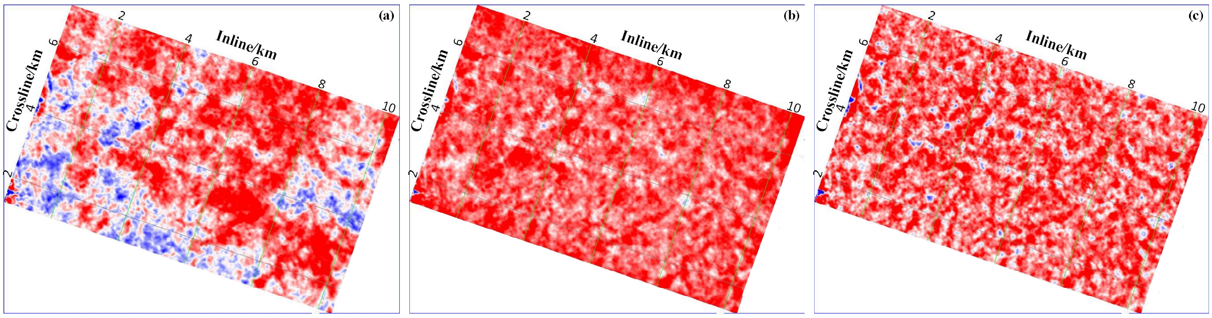

Figure 4: A time slice of the test result on raw seismic data from Eastern China. (**a**) Raw seismic data in deep layer in which weak-energy LGB waveform response is covered; (**b**) LGB seismic waveform response extracted by MCA-based method; (**c**) LGB seismic waveform response extracted by our method.

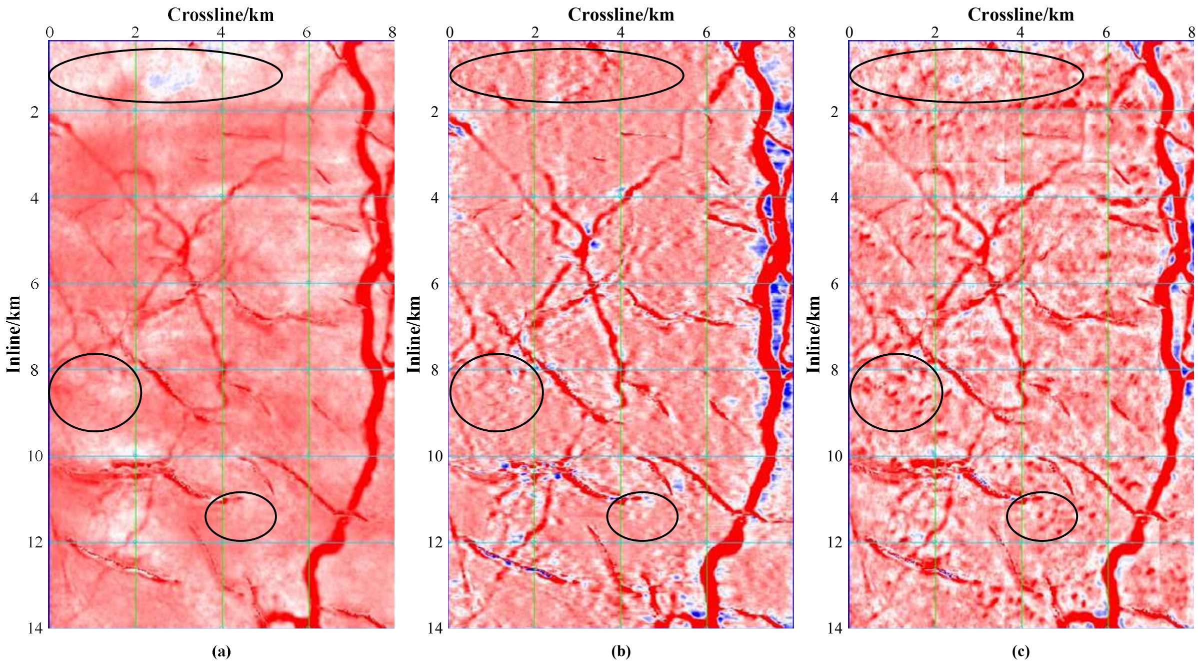

Figure 5: A time slice of the test result on another raw seismic data from Eastern China. (**a**) Raw seismic data; (**b**) LGB seismic waveform response extracted by MCA-based method; (**c**) LGB seismic waveform response extracted by our method.

REFERENCES

Araya-Polo, M., T. Dahlke, C. Frogner, C. Zhang, T. Poggio, and D. Hohl, 2017, Automated fault detection without seismic processing: The Leading Edge, **36**, 208–214, doi: 10.1190/tle36030208.1.

Chi, S., W. Chen, L. Zhang, D. Liu, and J. Chan, 2018, Three-dimensional seismic texture attributes analysis based on removed strong background noise: International Geophysical Conference, 418–421, doi: 10.1190/IGC2018-102.

Gao, D., 2003, Volume texture extraction for 3D seismic visualization and interpretation: Geophysics, **68**, 1294–1302, doi: 10.1190/1.1598122.

Haralick, R. M., and K. Shanmugam, 1973, Textural features for image classification: IEEE Transactions on Systems, Man, and Cybernetics, **6**, 610–621, doi: 10.1109/TSMC.1973.4309314.

Hart, B. S., 2008, Channel detection in 3-D seismic data using sweetness: AAPG Bulletin, **92**, 733–742, doi: 10.1306/02050807127.

Karbalaali, H., A. Javaherian, S. Dahlke, and S. Torabi, 2017, Channel boundary detection based on 2D shearlet transformation: An application to the seismic data in the South Caspian Sea: Journal of Applied Geophysics, **146**, 67–79, doi: 10.1016/j.jappgeo.2017.09.001.

Marfurt, K. J., and R. L. Kirlin, 2000, 3-D broad-band estimates of reflector dip and amplitude: Geophysics, **65**, 304–320, doi: 10.1190/1.1444721.

Mathewson, J., and D. Hale, 2008, Detection of channels in seismic images using the steerable pyramid: 78th Annual International Meeting, SEG, Expanded Abstracts, 859–863, doi: 10.1190/1.3063777.

Pham, N., S. Fomel, and D. Dunlap, 2018, Automatic channel detection using deep learning: 88th Annual International Meeting, SEG, Expanded Abstracts, 2026–2030, doi: 10.1190/segam2018-2991756.1.

Rumelhart, D. E., G. E. Hinton, and R. J. Williams, 1986, Learning representations by back-propagating errors: Nature, **323**, 533–536, doi: 10.1038/323533a0

Schwab, A., B. Cronin, and H. Ferreira, 2007, Seismic expression of channel outcrops: Offset stacked versus amalgamated channel systems: Journal of Petroleum Science and Engineering, **24**, 504–514, doi: 10.1016/j.marpetgeo.2006.10.009.

Simonyan, K., and A. Zisserman, 2014, Very deep convolutional networks for large-scale image recognition: arXiv preprint arXiv:1409.1556.

Suarez, Y., K. J. Marfurt, and M. Falk, 2008, Seismic attribute-assisted interpretation of channel geometries and infill lithology: A case study of Anadarko Basin Red Fork channels: 78th Annual International Meeting, SEG, Expanded Abstracts, 963–967, doi: 10.1190/1.3063798.

Wang, W., W. Chen, W. Liu, J. Xu, and J. Gao, 2011, Abrupt feature extraction via the combination of sparse representations: 81st Annual International Meeting, SEG, Expanded Abstracts, 1019–1024, doi: 10.1190/1.3627378.

Wu, X., 2017, Directional structure-tensor-based coherence to detect seismic faults and channels: Geophysics, **82**, no. 2, A13–A17, doi: 10.1190/geo2016-0473.1.

Zhao, T., 2018, Seismic facies classification using different deep convolutional neural networks: 88th Annual International Meeting, SEG, Expanded Abstracts, 2046–2050, doi: 10.1190/segam2018-2997085.1.